JAYCOR
3394 Carmel Mountain Road
San Diego, California 92121-1002
June 2001

Improving Accuracy of the F-Scan Sensor

Jaycor Technical Report 3150.32-01-143

Prepared by:
Bryant L. Sih, Ph.D.
JAYCOR

US Army Medical Research and Materiel Command

Contract No. DAMD17-00-C-0031

AD_____

Award Number: DAMD17-00-C-0031

TITLE: Modeling for Military Operational Medicine Scientific and Technical Objectives (Improving Accuracy of the F-Scan Sensor)

PRINCIPAL INVESTIGATOR: James H. Stuhmiller, Ph.D.
Bryant L. Sih, Ph.D.

CONTRACTING ORGANIZATION: Jaycor
San Diego, California 92121

REPORT DATE: June 2001

TYPE OF REPORT: Final

PREPARED FOR: U.S. Army Medical Research and Materiel Command
Fort Detrick, Maryland 21702-5012

DISTRIBUTION STATEMENT: Approved for Public Release;
Distribution Unlimited

The views, opinions and/or findings contained in this report are those of the author(s) and should not be construed as an official Department of the Army position, policy or decision unless so designated by other documentation.

20011005 289

REPORT DOCUMENTATION PAGE

Form Approved
OMB No. 074-0188

Public reporting burden for this collection of information is estimated to average 1 hour per response, including the time for reviewing instructions, searching existing data sources, gathering and maintaining the data needed, and completing and reviewing this collection of information. Send comments regarding this burden estimate or any other aspect of this collection of information, including suggestions for reducing this burden to Washington Headquarters Services, Directorate for Information Operations and Reports, 1215 Jefferson Davis Highway, Suite 1204, Arlington, VA 22202-4302, and to the Office of Management and Budget, Paperwork Reduction Project (0704-0188), Washington, DC 20503

1. AGENCY USE ONLY (Leave blank)	2. REPORT DATE	3. REPORT TYPE AND DATES COVERED
	June 2001	Final ( )

4. TITLE AND SUBTITLE
Modeling for Military Operational Medicine Scientific and Technical Objectives (Improving Accuracy of the F-Scan Sensor)

5. FUNDING NUMBERS
DAMD17-00-1-0031

6. AUTHOR(S)
James H. Stuhmiller, Ph.D.
Bryant L. Sih, Ph.D.

7. PERFORMING ORGANIZATION NAME(S) AND ADDRESS(ES)
Jaycor
San Diego, California 92121

E-Mail:

8. PERFORMING ORGANIZATION REPORT NUMBER

9. SPONSORING / MONITORING AGENCY NAME(S) AND ADDRESS(ES)
U.S. Army Medical Research and Materiel Command
Fort Detrick, Maryland 21702-5012

10. SPONSORING / MONITORING AGENCY REPORT NUMBER

11. SUPPLEMENTARY NOTES
Report contains color.

12a. DISTRIBUTION / AVAILABILITY STATEMENT
Approved for Public Release; Distribution Unlimited.

12b. DISTRIBUTION CODE

13. ABSTRACT *(Maximum 200 Words)*

14. SUBJECT TERMS

15. NUMBER OF PAGES
41

16. PRICE CODE

17. SECURITY CLASSIFICATION OF REPORT	18. SECURITY CLASSIFICATION OF THIS PAGE	19. SECURITY CLASSIFICATION OF ABSTRACT	20. LIMITATION OF ABSTRACT
Unclassified	Unclassified	Unclassified	Unlimited

Executive Summary

Recent advances in biomechanics have the potential to assist in the reduction of overuse injuries in the military. The three major components for this effort are: 1) a predictive overuse injury model, 2) a *portable* sensor to measure the primary input of the model—ground reaction forces, and 3) analysis of data from personnel undergoing military field exercises. This work evaluates the F-scan system as a potential sensor, specifically, its inability to accurately measure ground reaction forces. Modifications to make the F-scan system portable have been documented in another report (Sih 2001).

The F-scan system (Tekscan, Inc., Boston, MA) is a small in-shoe sensor that measures plantar pressure distribution using a thin disposable sheet composed of an array of pressure sensing elements or *sensels*. Previous studies have found that while the F-scan system is capable of accurately recording relative pressures, errors up to 62% in total load are possible (Luo et al. 1998; Sumiya et al. 1998). For example, using data from a military boot study (Harman et al.), unacceptable errors in the F-scan system were found when compared to a force platform (37±29% error at 3 selected points during the walking cycle).

This study examined the sources of error by analyzing the currently prescribed calibration method, characterizing the sensor both in and out of a shoe, and studying the long-term durability of the sensor. Because the sensor exhibits viscoelastic properties, part of the analysis involved fitting a standard linear solid (SLS) model to the results. It is believed that this is the first time the F-scan system has been modeled as a viscoelastic material.

In this study, the creep-like behavior of loaded sensels caused calibration errors that contributed to total load errors exceeding 30% during walking and running trials. However, sensor output was consistent from trial to trial. Isolating the sensor outside the shoe, the F-scan system behaved most similar to a spring during walking with the largest errors occurring during mid-stance, when the partial unloading of bodyweight resulted in sensor output that was lower than expected for an ideal spring. When the sensor was placed in the shoe, using the isolated sensor spring coefficient reduced errors but did not improve sensor accuracy to acceptable levels. Thus, the surface conditions inside the shoe had altered the F-scan sensor properties. However, using a set of coefficients derived from an in-shoe sensor under a wide range of gait speeds resulted in an SLS model that can reasonably approximate the plantar forces from an F-scan sensor output. Compared to Tekscan's prescribed calibration method, mean error was reduced from 31% to 11% using the SLS model.

Sensor longevity was also investigated and the results suggest that overuse causes the gap between the two load-bearing surfaces of a sensel to collapse. Once this occurs, the sensor no longer returns to zero output under zero load. The amount of time before the sensor becomes dysfunctional varies from sensor to sensor but it may be possible to develop models and criteria to account for the changes in the sensor before breakdown.

The results of this study indicate that the accuracy of the F-scan system is compromised by its viscoelastic behavior, causing errors during calibration and data collection. Applying a properly calibrated standard linear solid model to the F-scan output substantially reduces the error. This reduction may allow the collection of ground reaction forces accurate enough for predicting overuse injuries. The next step should be additional studies to confirm these results and to increase the complexity of the standard linear solid model to further improve on the F-scan accuracy.

Table of Contents

Introduction

A biomechanic analysis to aid in the reduction of overuse injuries in the military requires a portable force-recording device capable of measuring the ground reaction forces (GRF's) on the feet during different movements. Currently, GRF's are used to estimate many biomechanic variables that may be important in overuse injuries including energy expenditure, joint reaction forces, and muscle loads. Force platforms have traditionally been used to measure GRF's because of their high loading range and accuracy as well as their fast response time. However, force platforms are expensive and large, requiring a permanent or semi-permanent facility for a proper setup. Thus, most biomechanic analyses involve data collected from a laboratory in a controlled setting and complex movements such as those involving stairs, hills, and climbing have yet to be studied in detail outside the laboratory. The force platform/laboratory setting has also limited the biomechanic contribution to longer-term studies such as the analyses of daily activities, exercise regiments, and footwear because measuring GRF's for long periods in different environments is impractical with the force platform. Thus, to study overuse injuries over a wide range of movements there is a need for a portable sensor that can measure and record GRF's easily with a minimal hindrance to the subject. If such a system can be developed, it has the possibility of replacing the force platform, allowing the detailed analysis of the biomechanic causes of overuse injuries.

This report evaluates the F-scan system (Tekscan, Inc., Boston, MA) as a possible replacement for the force platform outside of the laboratory (Figure 1). F-scan is an in-shoe sensor that measures plantar pressure distribution using a thin disposable sheet composed of an array of pressure sensing elements or *sensels*. Patented ink within each sensel changes electrical resistance with load and a PC-based hardware and software package (currently at version 4.46) monitors the sensels, using a calibration scheme to convert the electrical resistance to pressure (see The Tekscan Prescribed Calibration Method, pg. 7). The F-scan A/D converter has a resolution of two bytes that can distinguish 256 levels of pressure. For convenience, this "raw" sensel data is referred to as *TekUnits*. With a sensel area of 25.8 mm^2, up to 954 sensels can be placed in a shoe, depending on foot size. In addition, the system is capable of collecting plantar pressure data up to 169 Hz. Modifications to make the F-scan system portable have been documented in another report (Sih 2001).

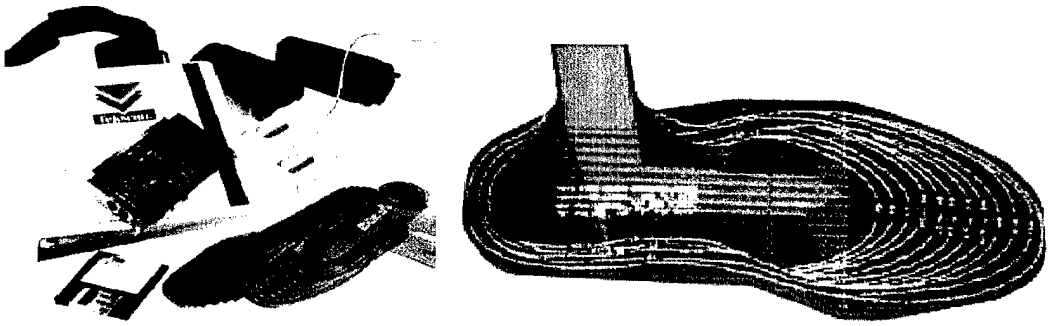

Figure 1. The F-scan System (Tekscan, Inc., Boston, MA). F-scan consists of a pair of foot sensors, a PCI A/D converter, and software (left image). The right image is a close-up of the sensor, revealing the layout of the 954 pressure sensels. (Source: www.tekscan.com)

Because F-scan can only measure pressure, one of the first concerns is the magnitude of the error from its in-shoe location. Converting plantar pressure data from F-scan to force is trivial (pressure × sensel area), but the resulting load is only the GRF component perpendicular to the plantar surface whereas a force platform measures three components of the GRF (vertical, anterior/posterior, and medial/lateral). However, during most human movements such as walking, the foot is flat against the ground during the majority of the load bearing phase, thus the plantar surface GRF closely mimics the vertical GRF commonly collected from a force platform (Figure 2). Because the vertical GRF is the dominant component (typically 4-5 times greater than the anterior/posterior and medial/lateral GRF's), a significant portion of the total GRF can be captured with either the vertical or F-scan derived plantar surface component.

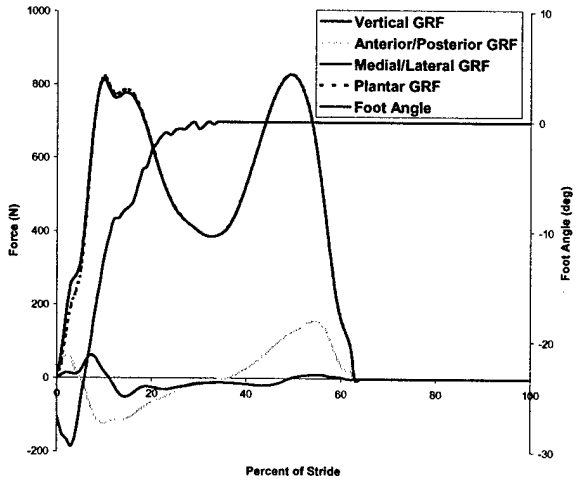

Figure 2. Comparison of the three ground reaction force components (GRF's) for walking measured from a force platform to the component plantar to the foot. Because the angle of the foot to the ground is small for most of stance, the difference between the vertical GRF and the plantar GRF is minimal.

In a recent study on the biomechanical differences between 12 boots (Harman et al.), in-lab GRF's were collected from both a force platform and an F-scan sensor, allowing a

comparison between the two methods. Although the F-scan calibration procedure was undocumented, it is clear that the results from the F-scan system were inconsistent. A sample of 20 trials shows an average error of 37±29% at 3 selected points during the walking cycle (Table 1). The magnitude and variability of the error may be too large for studies involving calculating the loads on the body such as bone stress for overuse injuries. For example, the error in vertical GRF from a single trial of the boot study would propagate through an inverse dynamics calculation, resulting in the same error magnitude in compressive force at the ankle (Figure 3). The results of the boot study show that while the F-scan system is capable, its overall accuracy needs to be improved before it can be an effective option for replacing the force platform.

Table 1. Mean ± SD error (i.e. difference) in the calibrated F-scan sensor output compared to a force platform for a sample of twenty trials from a military boot study (Harman et al.).

	Max Force Early Stance N / %	Min Force Mid Stance N / %	Max Force Late Stance N / %
Walking	-314 ± 230 / -36% ± 26	-159 ± 149 / -37% ± 34	-332 ± 236 / -39% ± 29

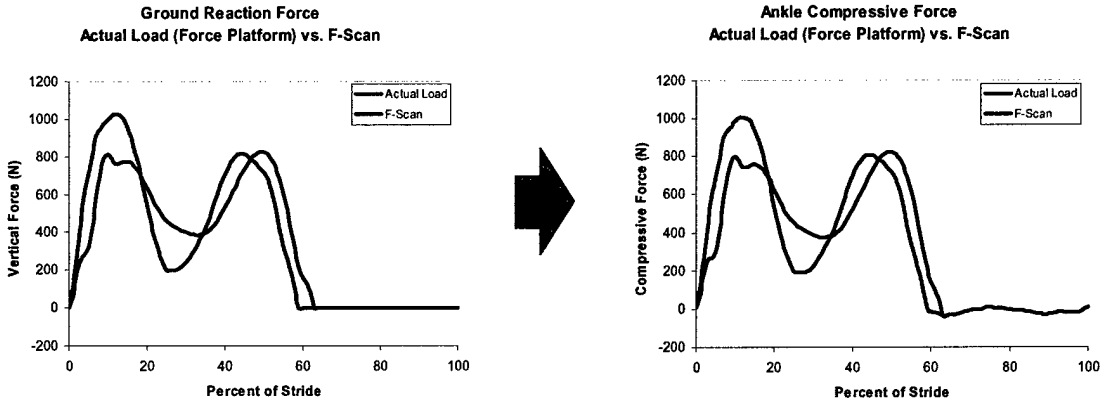

Figure 3. An example of how errors in the vertical GRF can affect results. Differences between the actual and the F-scan predicted load propagate through an inverse dynamics calculation to the compressive forces at the ankle.

The purpose of this study was to characterize F-scan as a total load sensor, suggesting ways to improve the current accuracy of the sensor, with the eventual goal of allowing it to replace the force platform in non-laboratory situations. To address this, the project focused on three areas: (1) critiquing of Tekscan's recommended calibration method of the F-scan system, (2) characterizing the F-scan sensor and improving on Tekscan's calibration, and (3) monitoring changes in the system with continued use. This is preceded by a brief literature review.

Literature Review

F-scan is gaining in popularity to assess plantar pressure distribution in diabetics and orthotic design (Saltzman et al. 1992; Novick et al. 1993; Albert and Rinole 1994; Mueller et al. 1994), but there have been relatively few studies characterizing the F-scan system. The following review briefly describes some of the F-scan characteristics reported in the literature.

Although the sensel response is approximately linear, studies have found that the total load reported by the sensels can vary by as much as 20% when compared to a force plate (Bauman et al. 1992; Mueller et al. 1994; McPoil et al. 1995; Woodburn and Helliwell 1996; Luo et al. 1998; Sumiya et al. 1998). A large portion of this variability can be attributed to F-scan's sensitivity to loading conditions. This includes soft surfaces and high loading rates, which have been found to reduce individual sensel output up to 62% even under controlled mechanical loading conditions (Luo et al. 1998; Sumiya et al. 1998). In addition, creep has been observed, making a static calibration difficult and the sensels were found to be temperature sensitive, especially at temperatures greater than 30° C (Luo et al. 1998; Sumiya et al. 1998).

During normal walking, Sumiya et al. (1998) found the total load predicted by F-scan compared favorably with force platform values during the first part of stance (93 to 101% of force plate values) but disagreed during the second half (14 to 17% reduction in predicted load). The study also found a delayed loading response (11 to 17% of total stance time). It should also be noted that the sensel pressure range is approximately 300-3000 kPa and appears to be more accurate at higher loads (Ahroni et al. 1998; Luo et al. 1998; Sumiya et al. 1998). However, pressures during normal walking are usually less than 120 kPa and some of the error could be caused by the sensor response in this low-pressure range. Because of these sensel characteristics, most studies recommend calibrating under the same temperature and loading conditions and conclude that F-scan is only reliable as a tool for comparing relative plantar distributions, as opposed to measuring absolute pressure values (Luo et al. 1998; Sumiya et al. 1998).

These studies suggest that while F-scan is capable of a linear response, the sensels exhibit creep and both a dynamic and temperature response consistent with a viscoelastic material. However, no studies have attempted to use a viscoelastic model to further increase the accuracy of the F-scan system. In addition, the wide range of errors reported suggest that calibration of the sensels is difficult and depends on the loading conditions. Thus, a reduction in F-scan error can also be made by improving the calibration procedure.

Examination of the F-scan Calibration Procedure and Sensor Output

The purpose of this experiment was to examine a typical F-scan calibration and sensor output, determine sources of error and establish a baseline with which to determine whether any improvements in the calibration/sensor output can be made. In addition, the repeatability of F-scan was investigated.

Methods

The Tekscan Prescribed Calibration Method

As prescribed by Tekscan, after conditioning the sensors (about 20 steps) to break-in a new sensor and to equilibrate the temperature with the foot and shoe, a two-step process for proper calibration was performed: an *equilibration* and a *calibration* step. Because each sensel is unique and may respond differently, an air bladder applied a uniform pressure across the entire sensor and each individual sensel was adjusted via Tekscan's software (i.e. equilibrated) to compensate for differences in outputs. While this may be important for pressure differences, in a preliminary study our results indicated that this correction is negligible for total load because the effect is averaged across a large number of sensels.

After equilibrating the sensor, the second part of Tekscan's calibration procedure involved loading the sensor with a known weight, usually body mass applied by standing on the sensor. Note that Tekscan recommends calibrating in the same manner in which it is being used. However, for dynamic measurements like walking, the load varies with time, making it impossible to calibrate "in the same manner" using their software and only a standing body weight was applied.

Experimental Methods

To assess the accuracy of the calibration method, two protocols were used. First, because the literature review indicated the sensor exhibits creep, a calibration was performed after 1-sec, 10-sec, and 60-sec of standing. After each calibration, four slow walking trials were collected. Second, using the 10-second calibration, four trials of slow walking, fast walking, and running were collected to see the influence of the calibration on different speeds. All trials were collected at 150 Hz for three seconds. Peak values at both the beginning and the end of stance as well as the minimum value during mid-stance were recorded. A force platform, synchronized and collecting at the same rate as the F-scan system, collected vertical GRF's for comparison.

It was assumed that the force platform values were correct and the difference between the F-scan sensor and the vertical component of the force platform GRF represented the error in the sensor. Both the absolute force (N) and percent difference (%) were calculated and the mean and standard deviation for each set of trials was reported.

The subject (male, 33 years, 67.7 kg) wore size 10.5 (US) casual dress shoes.

Results

Table 2. Mean ± SD error (i.e. difference) in the calibrated F-scan sensor output compared to a force platform at key points during gait. Increasing the time the sensor was loaded before calibrating resulted in greater errors in subsequent walking trials. The sensor always underestimated the load but the low standard deviation between trials shows the repeatability of the sensor output. Increasing gait speed also increased errors.

	Max Force Early Stance N / %	Min Force Mid Stance N / %	Max Force Late Stance N / %
Slow Walk- Time before calibration			
1 sec	-215 ± 46 / -27% ± 4	-109 ± 15 / -15% ± 2	-57 ± 8 / -11% ± 1
10 sec	-297 ± 11 / -37% ± 1	-209 ± 10 / -30% ± 1	-134 ± 5 / -27% ± 1
60 sec	-324 ± 9 / -43% ± 0	-255 ± 6 / -36% ± 1	-176 ± 13 / -36% ± 1
Gait Speed			
Slow Walk	-271 ± 9 / -34% ± 1	-133 ± 19 / -29% ± 4	-100 ± 25 / -14% ± 3
Fast Walk	-384 ± 21 / -44% ± 1	-142 ± 18 / -42% ± 4	-212 ± 11 / -26% ± 2
Run	-736 ± 85 / -42% ± 1		

In all trials, the Tekscan calibration resulted in F-scan underestimating the total load compared to the force platform, sometimes by as much as 44% (Table 2). However, the standard deviation for each protocol was low (usually less than 2%), showing the repeatability of the sensor output across different trials. Because of creep, longer times before calibrating resulted in higher TekUnit values being associated with the calibration load. This, in turn, caused F-scan to underestimate the total load during walking (Table 2). For a 664 N (67.7 kg) subject, a 1-minute calibration increased the error for the points tested an average of 125 N, or 19% of body mass compared to a 1-second calibration. In addition, the sensor output error varied for all gait speeds, with a better fit towards the end of stance (Figure 4). However, faster speeds (both walking and running) resulted in an increase in error (Table 2).

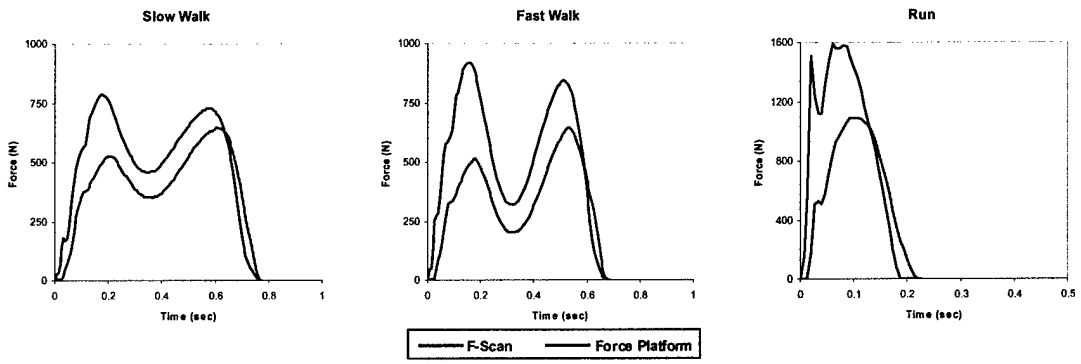

Figure 4. Three representative trials comparing the *in-shoe* F-scan to the force platform force for three different gait speeds. Note that the F-scan output comes closer in agreement with the force platform force at the end of stance (nonlinear response) and that some of the higher frequency peaks found in running have been attenuated. All speeds were tested using the same 10-second calibration.

Discussion

The calibration procedure prescribed by Tekscan assumes the sensor output follows a simple linear or spring-type model with a single coefficient to convert all sensel output to load or pressure. Calibration is basically a two-point calibration with the known load and measured TekUnits comprising one point and zero load/zero TekUnits comprising the second point. These two points are then used to generate the equation of a line, whose slope is the coefficient to convert TekUnits to pressure and load. Also, since the known load is applied unevenly (i.e. by the foot), only the total sum of all sensel TekUnits can be compared to the known load, meaning only a single coefficient is derived for all sensels.

The errors observed in this study were larger than those reported in literature (e.g. Luo et al. 1998; Sumiya et al. 1998) but were similar to the boot study (Table 1). They also depended on the amount of time calibrated, and the type of movement analyzed. It is unclear how most of the previous studies were able to consistently reduce the error in the F-scan output to less than 20% using Tekscan's prescribed calibration method. However, the overall "shape" of the sensor output was similar to the actual load and the low variability suggests that if F-scan can be calibrated correctly for the given conditions, the resulting load measurements will not only be accurate, but highly repeatable. Note that at higher gait speeds such as running, the slow response time of the sensor caused some higher frequency peaks to be missed, which may be important for some experiments.

Differences in the results because of differences in the calibration time can be explained by sensel creep (Figure 5). As a constant load is applied to a sensor (such as body mass), each sensel records a higher output with time. This effectively causes the calibration to underestimate the appropriate coefficient. Note that consistently performing a 1-second

calibration (smallest error) is difficult. It is an unreasonable amount of time for a subject to suddenly load the sensor without causing fluctuations.

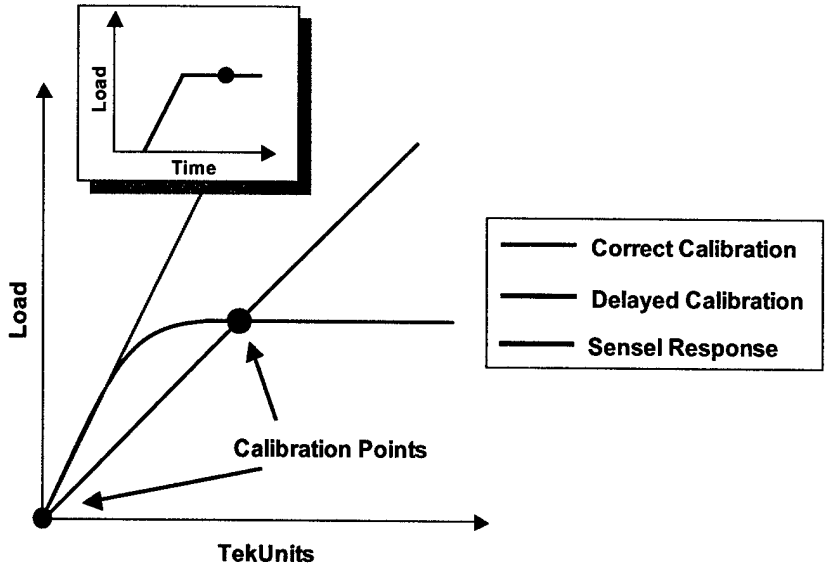

Figure 5. The effect of creep on the F-scan calibration. Because sensel output increases without a corresponding increase in load, a delay in calibration causes an underestimation of the slope or calibration coefficient.

These results also showed that the sensor behaves in a nonlinear creep-like manner, with a greater output during the later part of stance, even during short loading periods such as walking. Initially, it may appear that the shoe is "absorbing" some of the load during heel strike, thereby reducing the amount of load measured by F-scan. However, a free-body diagram of the shoe sole when the shoe is in contact with the ground (Figure 6) reveals that the load on the F-scan side be equivalent to the load on the force platform side because acceleration is minimal. Thus, the difference in F-scan output cannot be attributed to the shock attenuation properties of the shoe. (Any attenuation by the shoe would also reduce the external forces measured by the force platform.) Instead, the results suggest that the sensor is unable to accurately measure the load using the current calibration method.

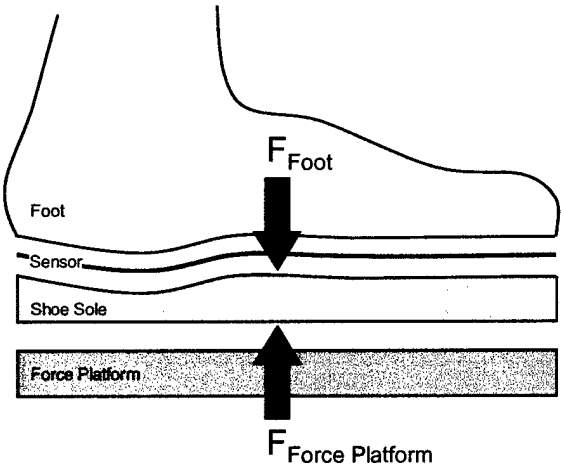

For the Shoe Sole:

$$\Sigma F = m \times a_0$$

$$F_{\text{Force Platform}} - F_{\text{Foot}} = m \times \cancel{a}^{0}$$

$$F_{\text{Force Platform}} = F_{\text{Foot}}$$

Figure 6. A free-body diagram of the shoe sole indicates that when the shoe is in contact with the ground and the acceleration of the sole is zero, the force measured by the force platform and the F-scan sensor are the same. Therefore, the nonlinear difference between the force platform and the sensor is due to a change in the properties of the sensor.

Conclusions

1. Errors greater that 20% are possible, even when following the prescribed calibration procedure.
2. Sensor output is repeatable from trial to trial.
3. Sensel creep leads to an underestimation of the calibration coefficient.
4. The sensor output is nonlinear, exhibiting creep-like behavior.

Modeling the F-scan Sensel Behavior

The results from the previous experiment indicate that a more detailed analysis of the in-shoe F-scan response is needed. However, it is unclear whether the observed responses were a result of the sensor or changes in the sensor because of the shoe environment. Therefore, the set of experiments in this section were designed to characterize the F-scan system in an isolated state *without* the shoe.

The most advantageous method to evaluate F-scan is to develop a viscoelastic model, relating the output from F-scan and the load applied, because this type of model has the capability of predicting a response to a wide range of loading conditions. Comparisons between the model's predicted load and the actual load indicate the error associated with the models as well as the level of improvement. To determine the most appropriate model, F-scan output was analyzed under a minimal set of variations (a single subject and shoe, primarily walking). It is assumed that additional subjects, shoes, and modes of gait can be analyzed to further refine the model in a later study.

Methods

Viscoelastic Models

While the F-scan output is a direct measure of the "sensel electrical resistance," it is assumed that this value is a reflection of the microscope changes in the distance between the two load-bearing sides of a sensel. Therefore, how this distance changes with load is the sensel response and because this change is dependent on the physical properties of the sensel, it can be modeled with a system of springs and dashpots. This enables one to derive an equation of motion, which predicts the sensor response to any load. For these initial experiments, a linear system was chosen, with a single coefficient characterizing the behavior of each spring and/or dashpot.

Two models were considered: a linear spring and a standard linear solid (SLS). The linear spring utilizes a single coefficient (load = $k \times$ distance; Figure 7A) and is identical to the coefficient of Tekscan's calibration procedure but will be chosen to minimize errors. The SLS is a spring and dashpot in parallel connected in series to another spring, requiring three coefficients to characterize the model (Figure 1B). This model was chosen because it exhibits both a spring and creep response yet still returns to its original resting state after the load is removed. (A simpler creep model that does not return to zero under no load is clearly incorrect.) Derivation of the equation of motion for the model can be found in Appendix A: Standard Linear Solid.

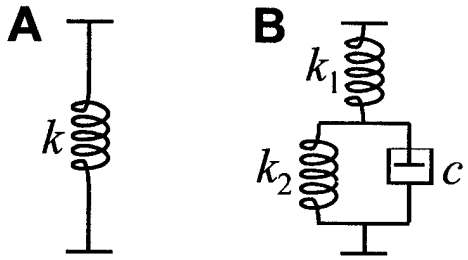

Figure 7. The two models considered for the F-scan system: (A) simple linear spring and (B) standard linear solid. The standard linear solid (SLS) exhibits creep, a known property of the F-scan system.

Experimental Methods

The F-scan sensor was taped to a force platform and a subject (male, 33 years, 67.7 kg) slowly walked barefoot across the sensor/force platform. Force platform data (N) and F-scan data (TekUnits) was collected at 150 Hz for three seconds and repeated four times. Peak values at both the beginning and the end of stance as well as the minimum value during mid-stance were recorded. Other modes of gait were not studied because of the difficulty in placing the foot on the sensor during testing.

Using each model's equation of motion, the *predicted load* was calculated from the model coefficients and the sensor outputs. This was compared to the force platform load (*actual load*) for each trial and the model coefficients were adjusted to minimize the root-mean-square error (rms) between the predicted and actual load in time. The model coefficients from four *calibration data* trials were averaged and applied to another set of four *independent data* trials to test the repeatability of the coefficients.

Results

The mean spring model coefficient was 0.15±0.00 N/TekUnit and the SLS coefficients were 0.20±0.01 N/TekUnit, 0.57±0.04 N/TekUnit, and 0.02±0.01 N-sec/TekUnit for k_1, k_2, and c, respectively (Table 3). The results were highly repeatable as shown by the low standard deviations. Interestingly, if the dashpot of the SLS model is small (e.g. when the sensor is loaded but the displacement is not changing), the resultant coefficient of the two springs is 0.15 N/TekUnit, a value very similar to the spring model coefficient.

Table 3. The viscoelastic model coefficients from the four *calibration* trials used to determine the mean coefficient values. Coefficients were derived for each trial by minimizing the root-mean-square (rms) error between the actual and the predicted model loads.

Experiment #1	Spring		Standard Linear Solid			
	k N/TekUnit	rms N	k_1 N/TekUnit	k_2 N/TekUnit	c N-sec/TekUnit	rms N
Trial a	0.15	47.68	0.20	0.57	0.02	41.70
Trial b	0.14	49.75	0.20	0.51	0.02	38.69
Trial c	0.15	50.62	0.18	0.58	0.03	42.16
Trial d	0.15	45.19	0.20	0.60	0.02	36.73
mean	**0.15**	48.31	**0.20**	**0.57**	**0.02**	39.82
sd	0.00	2.42	0.01	0.04	0.01	2.57

Comparing the predicted and actual load, both the spring and SLS model were able to convert the F-scan output to load with reasonable accuracy (Table 4, Experiment #1) with most error occurring during mid-stance (~8% error). Using both models (with their mean coefficients) on the independent set of data resulted in slightly greater errors on average (6.2% versus 4.5% for the values measured). However, from the data (Table 4, Experiment #2) it is apparent that the SLS model's accuracy has decreased more than the spring model's. Again, most error occurred during mid-stance. Overall, however, both models appeared to follow the actual load closely (Figure 8).

Table 4. Using the mean coefficient values from Table 3, the error in the model predictions were compared to the actual load during slow walking with the F-scan sensor taped to the force platform. Because the coefficients were derived from Experiment #1 (calibration data), there were smaller errors seen in this data set. Using the coefficients on the independent set of data (Experiment #2) results in slightly more error and variability, mainly for the SLS model.

	Max Force Early Stance N / %	Min Force Mid Stance N / %	Max Force Late Stance N / %
Experiment #1			
Spring	-32 ± 20 / -5% ± 3	43.25 ± 8 / 8% ± 1	-13.75 ± 7 / -2% ± 1
Standard Linear Solid	-18 ± 9 / -3% ± 1	35.5 ± 7 / 7% ± 1	-12.25 ± 6 / -2% ± 1
Experiment #2			
Spring	-29 ± 31 / -4% ± 5	45 ± 29 / 8% ± 5	25 ± 48 / 4% ± 7
Standard Linear Solid	27 ± 52 / 4% ± 8	76 ± 49 / 14% ± 9	18 ± 20 / 3% ± 3

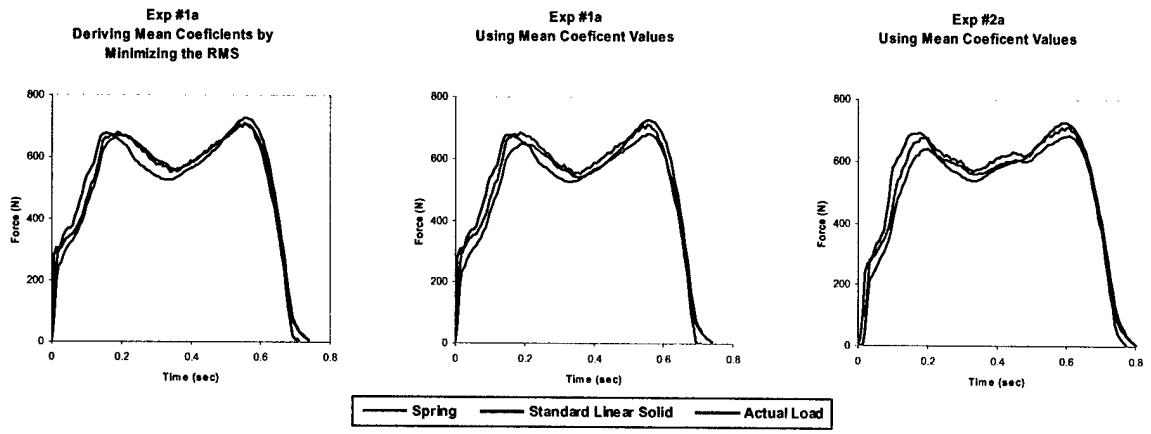

Figure 8. Three representative trials comparing the spring and SLS predicted loads to the actual loads during slow walking with the F-scan sensor taped to the force platform. The left graph shows a single calibration trial's spring and SLS output whose coefficients had been chosen to minimize the error with the actual load. Four of calibration trials were collected. The middle graph shows the output from the same trial using the mean coefficient values from the calibration trials. The right graph shows the output from an independent trial using the mean coefficient values. These plots demonstrate the consistency of the models for a given subject and walking speed.

Discussion

Looking at the overall shape and error, both the spring and SLS model were able to reasonably recreate the actual load from the F-scan data when the sensor is taped to the force platform. Compared to the SLS model, the spring model had slightly higher errors when the mean coefficients were reapplied to the calibration data but the error did not increase appreciably when applied to the independent data. Also, because the spring coefficients of both models result in a similar response at low loading rates, it is apparent that the dashpot of the SLS model had the largest effect during the initial part of stance when rates were high (Figure 8). However, the dashpot also appeared to increase errors in the independent data suggesting that it is more sensitive to subtle differences in loading conditions than the spring model. This indicates that while the SLS model is capable of recreating the actual load, the true nature of the F-scan sensel is not accurately portrayed by the SLS model. It is doubtful whether this model would function well under these experimental conditions with a wide range of loads.

Mid-stance had the greatest error indicating that neither model was capable of reproducing the partial unloading phase of gait particularly well. Looking closer at this region of the data, it is apparent that the number of TekUnits for the actual load is too low for either model, suggesting that the F-scan behavior is different during unloading. However, the overall result of both models is reasonable and a more complex model designed to capture this part of gait was not attempted.

The results indicate that while the SLS model is able to more closely match the calibration data, this model is more sensitive and does not appear to be as reliable. Thus, the spring model appears to be the most appropriate model for an isolated F-scan sensor. Although this is the same model utilized by Tekscan, because the force platform calibrates the sensor during walking (as opposed to just standing on the sensor), the results closely matched an actual walking trial. Note that the *in-shoe* results presented earlier (Figure 4) indicate that the spring model will have to be modified with additional nonlinear terms in order to predict the sensor response in the shoe environment.

Conclusions

1. Both the spring and SLS model were able to reasonably recreate the actual load from the F-scan data when the sensor was isolated (i.e. taped to the force platform and not in a shoe). Errors less than 10% were seen.

2. The dashpot of the SLS model improved the model response during rapid loading but contributed to more errors and variability during the rest of stance.

3. Lower than expected TekUnits during mid-stance caused the partial unloading phase to have the largest errors. Neither model was able to adjust for these errors.

4. The sensitivity of the SLS model suggests that the spring model is more robust and the appropriate model for these experimental conditions.

Adapting the Model for In-Shoe Sensing

While the previous experiment highlighted the spring model as the best model for an isolated F-scan sensor, it is clear from the preliminary in-shoe results (Figure 4) that in a different environment the sensor also behaves in a nonlinear manner. The most likely cause for the nonlinear behavior is surface hardness of the shoe insole. Unlike the isolated or *out-of-shoe* sensor testing, the foot is applying a non-uniform load to a shaped, pliable insole surface, deforming the sensor unevenly. Although the overall load is still directly comparable to the external force platform load (Figure 6), these deformations are somehow changing the characteristics of the F-scan sensor.

To account for these changes, two sets of experiments were performed. One set assumed that the spring model derived from the isolated testing could be directly adapted using three empirical modifications: a gradient-dependent spring coefficient, a derivative-dependent spring coefficient, and a standard linear model (SLS) with a fixed spring coefficient. The unmodified spring coefficient for all the models was chosen to be 0.15 N/TekUnit, the value derived from the isolated sensor experiments described previously.

To see if further improvements could be made, a second experiment reanalyzed the sensor using the same methods as the out-of-shoe tests (a spring and SLS model), deriving a new set of coefficients not based on the isolated sensor tests. The purpose was to investigate how the spring coefficient changes with gait speed and to see if a single SLS model, which may be effective because of its viscoelastic nature, could be used for different gait speeds.

Because the purpose of these models is to increase the accuracy of the F-scan system during different modes of gait, three gait speeds were tested: slow walking, fast walking, and running. As before, comparisons between a model's predicted load and the actual load indicate the error. In addition, because these new models are based on a sensor's response in a specific shoe environment, it is assumed that each new shoe and subject will have to be tested prior to use.

Methods

Empirical Models

For the gradient- and derivative-dependent models, the spring coefficient was modified as follows. From the previously described equation for a spring, the total load is the product of the output of all sensels and the spring coefficient (k),

$$\text{Total Load} = \sum k \cdot \text{TekUnit}_i$$, where i represents an individual sensel.

The modification for the new set of experiments assumed that another term based on the spring coefficient could describe the changes to the sensel output:

$$\text{Total Load} = \sum (k \cdot \text{TekUnit}_i + \alpha \cdot \Delta_i \cdot k \cdot \text{TekUnit}_i)$$

where

Δ_i = the absolute gradient or derivative at sensel i

α = model coefficient.

For the gradient-dependent model, Δ_i is the magnitude of the gradient vector in TekUnits between an individual sensel and it's neighbors. For the derivative-dependent model, Δ_i is the change in sensel TekUnits per time, calculated using a finite difference algorithm.

Referring to the diagram in Appendix A: Standard Linear Solid (Figure 15), the standard linear solid model assumed that the series spring (k_1) represented the sensor, thus having the same value as the spring model coefficient, k. The remaining spring and dashpot (k_2 and c) were assumed to represent the material properties of the shoe.

Experimental Methods

The F-scan sensor was placed in a subject's shoe and an appropriate amount of time was given for the sensor to equilibrate and settle in the shoe. The subject (male, 33 years, 67.7 kg) walked at three different gait speeds: slow walk, fast walk, and run. Force platform data (N) and F-scan data (TekUnits) was collected at 150 Hz for three seconds and repeated four times for each gait speed.

In the first set of experiments, the gradient, derivative, and SLS model's coefficients were chosen to minimize the root-mean-square (rms) error between the model and the force platform load at each gait speed. In all cases, k (or k_1 for the SLS model) was 0.15 N/TekUnit, the value derived from the previous experiment. To assess the accuracy of the models, the difference between the force platform and the model output was calculated at three points in the gait cycle: peak force during early-stance, minimum force at mid-stance and peak force at the end of stance. For running, only a single peak force was recorded. Mean and standard deviations for each gait speed and model were calculated.

The second set of experiments involved deriving three separate best-fit spring coefficients (one for each gait speed) as well as an average set of coefficients for a SLS model used at all gait speeds. This was accomplished by minimizing the rms between the models and the force platform. As before, the model accuracy was assessed at specific points in early-stance, mid-stance, and late-stance using mean and standard deviation values.

Results

In general, the first set of experiments revealed that with a model utilizing a single primary spring (k = 0.15 N/TekUnit), errors increased with gait speed. The three models that modify the spring failed to substantially improve the results, in both magnitude and variability (Table 5). The largest errors occurred during early-stance (-19±6%), followed by mid-stance (-15±8%) and late-stance (5±7%).

Table 5. The error in four model predictions compared to the actual load during gait at different speeds with the F-scan sensor inside the shoe. All models contained a primary spring whose value (k = 0.15 N/TekUnit) was derived from out-of-shoe testing (Table 3). Even though each gait speed had a unique set of non-spring coefficients that minimized the error, only the gradient-dependent model showed any improvement over the spring model. Error was calculated at 3 points of gait (early-, mid-, and late-stance).

	Slow Walk N / %	Fast Walk N / %	Run N / %
Spring Only (k = 0.15)	-13 ± 89 / -2% ± 12	-106 ± 93 / -17% ± 11	-372 ± 151 / -21% ± 8
Gradient-dependent Spring	-38 ± 74 / -6% ± 16	-49 ± 118 / -9% ± 16	-137 ± 13 / -8% ± 1
Derivative-dependent Spring	-20 ± 82 / -3% ± 12	-296 ± 94 / -16% ± 12	-296 ± 136 / -17% ± 7
Standard Linear Solid	-47 ± 68 / -8% ± 11	-106 ± 93 / -17% ± 11	-381 ± 132 / -22% ± 7

The gradient-dependent model showed a minor but noteworthy improvement in accuracy relative to the spring model (Table 5). Referring to Figure 9, for some slow walk trials the gradient-dependent model was able to account for the nonlinear sensor behavior by reducing the effective spring coefficient during late-stance. In addition, a few running trials were improved because the gradient increased the effective spring coefficient. However, the high variability of the gradient-dependent results, especially at walking speeds, is a reflection of this model's tendency to underestimate the load during early-stance and overestimate the load during late-stance (e.g. Fast Walk of Figure 9).

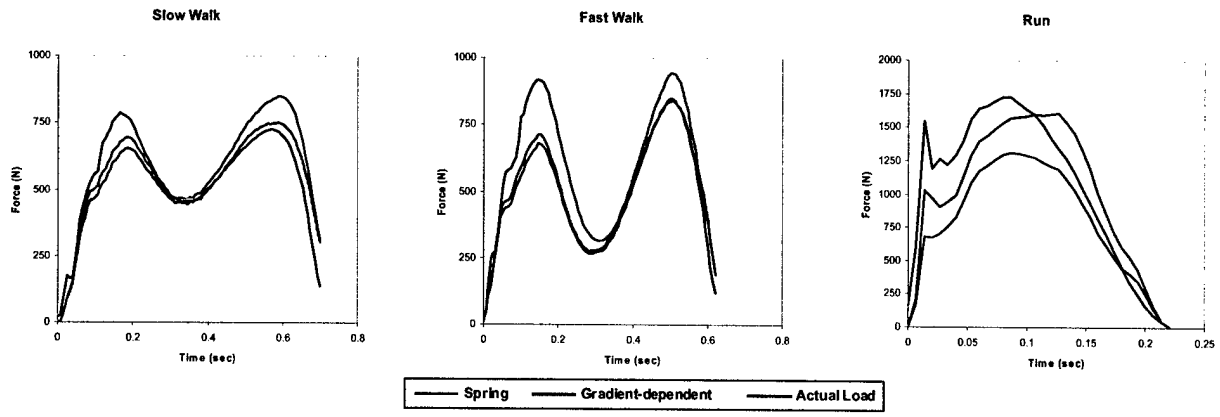

Figure 9. Three representative trials comparing the spring and gradient-dependent predicted loads to the actual loads during three gait speeds with the F-scan sensor inside the shoe. Both models are unable to duplicate the force profile well, especially during early-stance. Note that large gradients during late-stance for slow walking allow the gradient-dependent model to more closely match the actual load during this phase. Using a different gradient-dependent coefficient, this model is also able to more closely match the actual load during running.

In the second set of experiments, as speed increased the best-fit spring coefficients increased from 0.15 to 0.19 N/TekUnit, resulting in smaller errors than the previously tested in-shoe models with the fixed coefficient. Using coefficients of k_1 = 0.19 N/TekUnit, k_2 = 0.0001 N/TekUnit, and c = 0.31 N-sec/TekUnit, the best-fit SLS model also showed a reduction in errors compared to the fixed coefficient models. Both of these trends can be seen by comparing Table 6 to Table 5. Although the SLS model was not as good as the best-fit spring model, the errors were comparable with a notable improvement by the SLS model during early-stance (-4±7% vs. -15±2%). However, the SLS model increased error during mid-stance (-17±13% vs. -9±7%). Overall, both models are better equipped to predict total load over a wide range of gait speeds than the fixed coefficient models presented earlier (Figure 10).

Table 6. The error in two model predictions compared to the actual load during gait at different speeds with the F-scan sensor inside the shoe. The spring model used three different spring constants chosen to minimize the rms for a given gait speed. The SLS coefficients were unchanged between gait speeds and were chosen to minimize the rms for all gait speeds tested. Error was calculated at 3 points of gait (early-, mid-, and late-stance).

	Slow Walk N / %	Fast Walk N / %	Run N / %
Spring (k_{slow} = 0.15, k_{fast} = 0.17, k_{run} = 0.19)	-13 ± 88 / -2% ± 12	-30 ± 100 / -6% ± 13	-6 ± 165 / 0% ± 10
Standard Linear Solid (k_1 = 0.19, k_2 = 0.0001, c = 0.31)	27 ± 58 / 3% ± 9	-47 ± 73 / -11% ± 15	-62 ± 170 / -3% ± 10

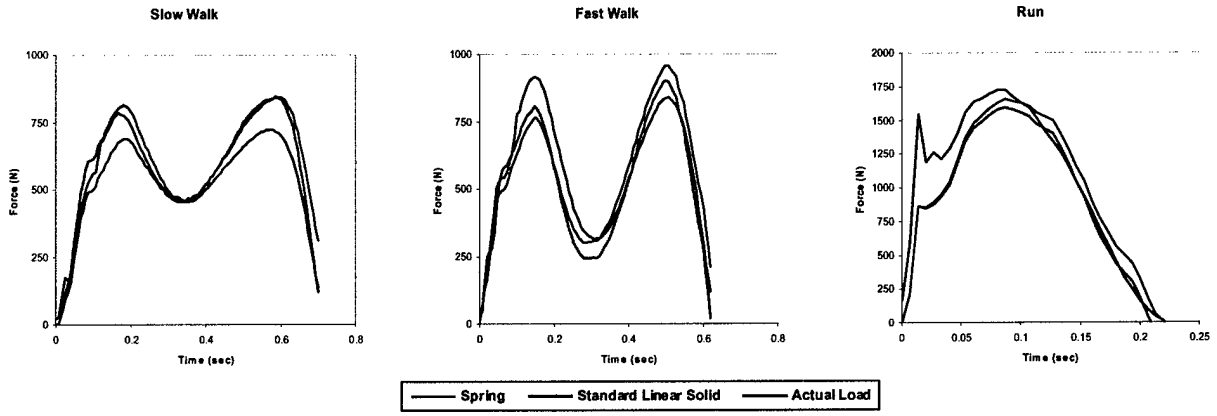

Figure 10. The same three representative trials as in Figure 9 comparing an optimized spring and SLS model to the actual load. The spring model uses coefficients of 0.15, 0.17, and 0.19 N/TekUnit for the slow walk, fast walk, and run, respectively. The SLS model uses coefficients of k_1=0.19 N/TekUnit, k_2=0.0001 N/TekUnit, and c=0.31 N-sec/TekUnit. A detailed description of the SLS model can be found in Appendix A: Standard Linear Solid.

Discussion

Compared to both the boot study data (Table 1) and the Tekscan calibrated results (Table 2), the fixed spring coefficient models were clearly an improvement (Table 6). However, only the gradient-dependent model appeared to further improve the spring model by accounting for some of the nonlinear behavior under certain circumstances. Thus, it appears that while the gradient may be a factor in the sensor behavior, the form of the empirical model utilizing the gradient is not exact. Because the effect of the gradient seems to depend on gait mode (it reduces the spring coefficient during walking but increases the coefficient during running), a better understanding of the effect is needed before it can be successfully incorporated into a model.

In the second set of experiments, the best-fit spring coefficient increased with gait speed, supporting the results that a single spring coefficient is insufficient to properly model the sensor. However, if a separate coefficient is used for different gait speeds, errors were reduced substantially. Of course, the nonlinear aspect of the output cannot be addressed by this simple spring model.

The SLS model also reduced the error at different gait speeds substantially, and having a single set of coefficients for all gait speeds gives this model a distinct advantage over the spring model. The robustness of the SLS model indicates that it has captured the sensor behavior at least to first-order and has the ability to reasonably reproduce the vertical/plantar GRF for a large range of gait speeds. However, despite its nonlinear behavior, the SLS model did not improve the accuracy or consistency of the sensor compared to a best-fit spring for a given gait speed. Part of this is due to the model's inability to return to

a resting state immediately after no load because of the dashpot. This indicates that a more complex model in needed, with higher-order springs and dashpots that are capable of reproducing the observed behavior. It should be noted that the equations of motion of more detailed models are often too complex to derive a closed-form solution and instead require advanced numerical methods to approximate their behavior.

The results of this study also suggest the direction for model development. The primary spring coefficient (k_1) was 0.19 N/TekUnit, the same value as the best-fit spring model for running. Also, the second spring (k_2) was small, with only enough value to eventually return the model to its original resting state with no load. Thus, the overall behavior of the remaining dashpot is to both reduce the spring behavior during slow movements such as walking and to account for the nonlinear sensor output. It is likely that separating these two characteristics of the sensor with additional dashpots (or a more complex one) will further improve this model. In addition, the errors during mid-stance strongly suggest the sensor behaves differently during unloading and a different dashpot coefficient should be used during this time. Also, because the current scope of the study was limited to a single subject/shoe combination, additional model development and an increase in the number of testing protocols should lead to further improvements in the F-scan system.

Conclusions

1. The surface conditions inside the shoe alter the F-scan sensor output.
2. The sensor may be sensitive to gradient but the relationship to sensel output is unclear.
3. The response of the sensor changes with gait speed.
4. Although variability is high, using a set of coefficients derived from a wide range of gait speeds results in an SLS model that can reasonably approximate the plantar forces from an F-scan sensor output. Mean errors were less than 11%.
5. Additional subjects, shoes, and gait speeds as well as a more complex model will likely further improve the F-scan accuracy.

Long Term Changes in F-Scan Output

Another concern of the F-scan system is its ability to record GRF's for an extended period of time. While the previous experiments have demonstrated that the sensor could be successfully calibrated for a wide range of gait speeds, for GRF's to be easily collected outside the laboratory, the sensor's long-term creep (Luo et al. 1998; Sumiya et al. 1998) and eventual failure from overuse (McPoil et al. 1995) need to be addressed. Moisture has also been known to accelerate the breakdown of the sensor (Ahroni et al. 1998). It is clear that the longevity of the sensor is a complex problem and the purpose of this section is to examine the long-term changes in the F-scan sensor in order to get a better understanding of these issues.

Methods

Because it was impractical and premature to expose the sensor (and subject—male, age 33, 67.7 kg) to a strictly controlled long-term gait regiment, the sensor was placed in the shoe and recorded during the subject's normal daily activities (office work with occasional short walks). Three separate sensors were tested (#1, #2 and #3). After the usual break-in regiment, each sensor's output (TekUnits) was collected at 150 Hz for three seconds with the subject walking slowly. Force platform data (N) was also collected at the same time. Data was collected at short intervals (2-3 minutes apart) for the first ten minutes and increased to approximately one collection every hour. Sensors were worn for three to five hours.

Using the methods described previously, a standard linear solid model (SLS) was fit to the first walking trial of each sensor (time = 0:00) and used to calculate the predicted load for each subsequent trial. Key values at early-stance, mid-stance, and late-stance were compared to the force platform. Mean and standard deviations as a percentage of the force platform load for each trial was collected.

Results

In general, the structures maintaining the gap between the two surfaces of an F-scan sensor collapsed with overuse, causing the surfaces to maintain contact continuously. Moisture, entering from the exposed edges of the sensor because it was trimmed to fit in the shoe, appeared to exasperate the problem, causing the sensor surfaces to stick together more easily. This resulted in a sensor whose output failed to return to zero under no load. This occurred mainly in the heel portion of the sensor, where the load was distributed over a smaller area (higher pressures) than when the force was on the forefoot (Figure 11).

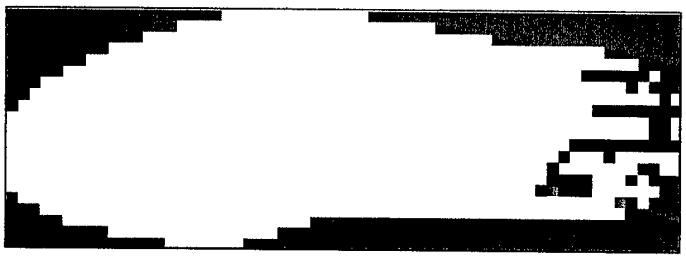

Figure 11. An F-scan sensor with heel damage from overuse. Because the integrity of the sensor has been compromised, the load bearing sides of some sensels remain in contact, resulting in an output even without load.

Even though the stuck surfaces in all three sensors appeared similar, two different responses were observed. In two of the sensors (#1 and #2), the output increased, causing the SLS model to overestimate the actual load with time. In addition, the zero load output due to collapsed sensors increased to over half of the peak load. This is most evident at the start of stance of the final trial in Figure 13, where the actual load is near zero but the SLS model predicts 417 N. In contrast, the output of Sensor #3 changed so that the model underestimated the actual load by 26% after three minutes. However, the error stabilized quickly, with the average ranging from -20% to -25% for the first 2.75 hours. By 3.75 hours, the error had only decreasing to -30% (Figure 12). The number of collapsed sensels was smaller in this sensor as well, resulting in the model under predicting the load by only 45 N at the start of the final trial (Figure 14).

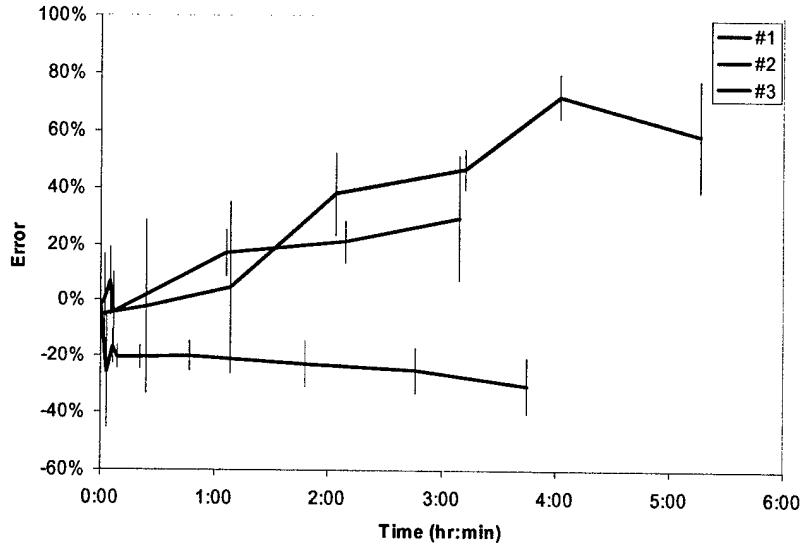

Figure 12. Error in three F-scan sensors during walking compared to a force platform over an extended period. Two different types of behavior were seen: a creep-like behavior (#1 and #2) and a loss of sensitivity (#3).

It should also be noted that the SLS model of Sensor #3 was able to duplicate the shape of the actual load more accurately. Comparing Figure 13 to Figure 14, it is apparent that

the SLS model for Sensor #3 only required an increasing spring coefficient with time; the model preserved the overall "shape" of the actual load for about three hours. Sensors #1 and #2, on the other hand, often exhibited erratic behavior as the sensor degraded.

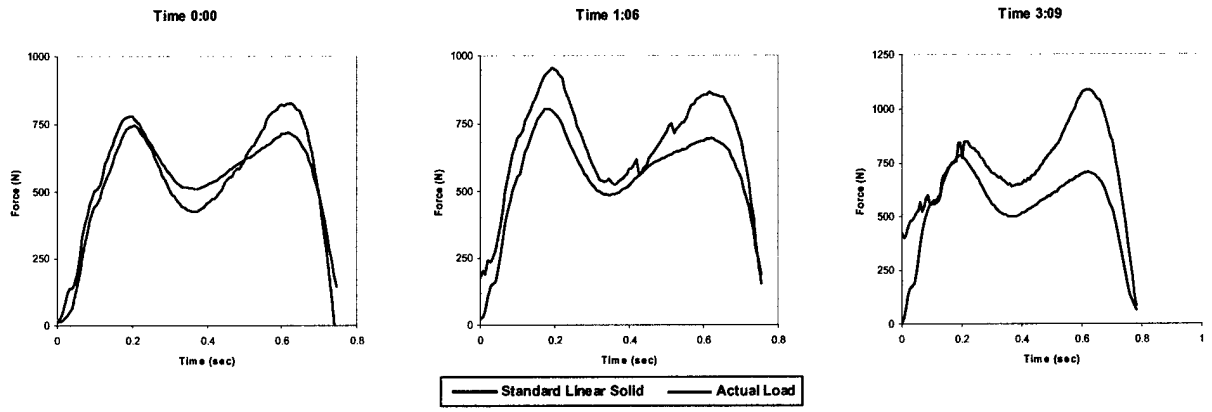

Figure 13. Representative trials from a long-term test showing creep-like behavior. Note the irregular pattern that developed in the SLS output as well as the large offset at the start of stance as individual sensels became defective.

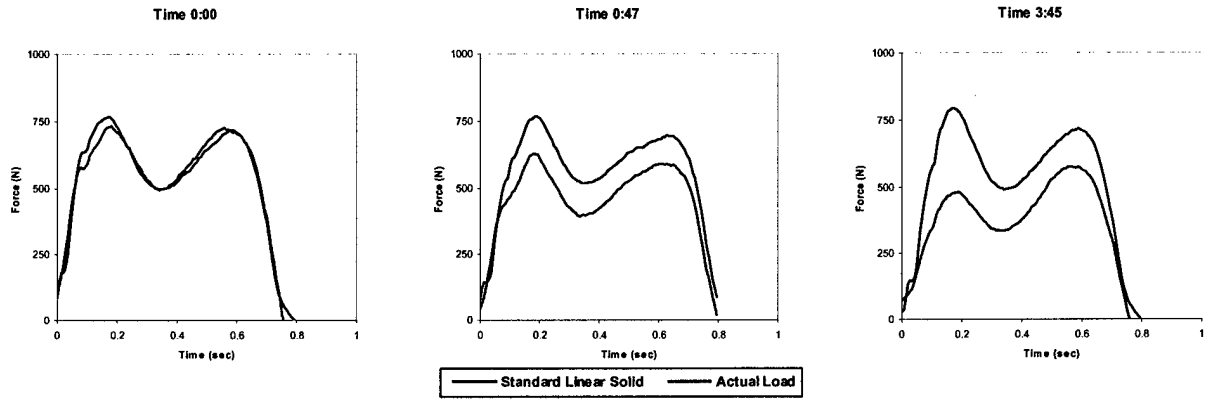

Figure 14. Representative trials from a long-term test showing a loss of sensitivity. Note the behavior of this sensor is different, with the SLS model approximating the actual load well for except for an increasing offset for most of the test. It is not until the end of the experiment (time = 3:45) that the SLS predicted load begins to resemble the other two sensors, with an increased predicted load occurring during late-stance compare to early-stance.

Discussion

Although it is difficult to derive any specific conclusions from only three sensors, the sensor responses suggest that the properties of the material separating the two sides of a sensor vary, allowing some sensors to last longer than others. Sensor #3 appeared to need a few more minutes to stabilize but after this added time, the sensor was functional for an extended period of time. In this study, another three hours were required before the output begun to resemble the output from the first two sensors, where an increased predicted load occurred during late-stance compared to early-stance (Figure 14). (It is unclear whether

Sensor #3's response would have followed the other sensors if the test time was extended.) If further studies confirm that some sensors are more "robust," then it may be desirable to develop a method to identify these sensors. In addition, while Sensor #1 and #2 degraded more quickly, the rate appears to be linear. Thus, another option is to develop a more complex SLS model that can account for these errors over an extended period. Again, more tests will determine which direction is more appropriate. This experiment also revealed that moisture could affect sensor longevity and it may be necessary to re-seal the edges of the sensor after trimming.

Conclusions

1. Sensor longevity is dependent on maintaining the gap between the two surfaces of a sensel.
2. When the gap collapses from overuse, the sensor output no longer returns to zero under no load.
3. The amount of time before the sensor becomes dysfunctional varies from sensor to sensor.
4. It may be able possible to develop models and criteria to account for the changes in the sensor before breakdown but additional studies are needed.

Conclusions

Although more research is needed to confirm the results of this study, the data indicates that with a few modifications, the F-scan system is capable of recording the plantar GRF outside the laboratory. It is clear that the environment (i.e. shoe and gait profile) plays an important role in changing the behavior of the sensor. While this study did not attempt to explain the causes of these changes, the primary modification recommended is to revise the calibration procedure prescribed by Tekscan. Rather than a "static" calibration where the subject stands on the sensor, the use of a force platform for a "dynamic" calibration in conjunction with the standard linear model yields much better results over a wide range of gait speeds (4-10× increase in accuracy). The reduction in sensor error from the boot study (Harman et al.) and Tekscan calibration through the spring and SLS models highlight the improvements made in calibrating F-scan sensor output through modeling (Table 7). However, the SLS model does not improve the variability appreciably and the current scope of the study was limited to a single subject/shoe/step combination.

Table 7. A summary of the progression of the F-scan sensor accuracy due to model improvements (% error relative to a force platform) for three gait speeds.

	Slow Walk	Fast Walk	Run
Previous Study	%	%	%
Boot Study I (Harman et al.)	---	-37% ± 29	---
Current Study			
Tekscan Calibration	-26% ± 9	-37% ± 9	-42% ± 3
Spring (k = 0.15)	-2% ± 12	-17% ± 11	-21% ± 8
Optimized Standard Linear Solid	3% ± 9	-11% ± 15	-3% ± 10

Despite the overall improvement of the F-scan output because of the enhanced calibration procedure, additional issues will need to be addressed before the sensor is able to fully replace the force platform. An obvious area is further development of the SLS model. The research from this study indicates that a viscoelastic model that has been modified to properly reproduce the unloading behavior of the F-scan system will further increase accuracy, especially during mid-stance and the end of stance. In addition, while the overall creep behavior of the sensor can be characterized by a linear dashpot, the data from this study clearly indicates a more complex function is necessary. Also, the model's response to multiple steps will need to be investigated.

While not critical, understanding the factors affecting longevity of the sensor will be important for long-term studies such as overuse injuries. The two different sensors responses seen in this report will have to be confirmed, but the preliminary data suggest that either response can be quantified, allowing adjustments to the F-scan output.

One issue that has not been address by this study is the ability to reproduce the remaining GRF components (medial/lateral and anterior/posterior) from the F-scan system. Although the current sensor only measures one component of load, using other information such as body weight and previously collected GRF's, it may be possible to reconstruct the entire force profile. Other researchers have identified this problem and have begun developing neural networks to predict the remaining GRF's from insole pressure patterns (Savelberg and de Lange 1999). If such a technique is successful, reconstructing the entire GRF profile should be feasible.

Appendix A: Standard Linear Solid

The standard linear solid (SLS) consists of a spring and dashpot in parallel connected in series to another spring (Figure 15). This type of model exhibits both creep (deformation at a constant load) and stress relaxation (reduced stress at a constant deformation).

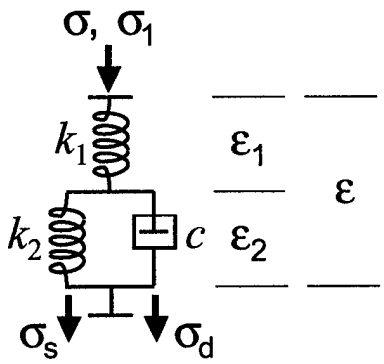

$$\varepsilon = \varepsilon_1 + \varepsilon_2$$
$$\sigma = \sigma_1 = \sigma_s + \sigma_d$$
$$\sigma_1 = k_1 \cdot \varepsilon_1$$
$$\sigma_s = k_2 \cdot \varepsilon_2$$
$$\sigma_d = c \cdot \dot{\varepsilon}_2$$

Figure 15. The standard linear solid consists of a spring and dashpot in parallel connected in series to another spring (left). Using the model's fundamental equations (right), the complete load-displacement response of the model can be calculated.

Assuming that the load on both springs (σ_1, σ_s) is linear with respect to the spring's local displacement (ε_1, ε_2) and the load on the dashpot is linear with respect to the change in displacement or velocity ($\dot{\varepsilon}_2$), one can derive the equations in Figure 15 to completely describe the response of the model. Combining the equations and solving for the overall load and displacement results in the following differential equation:

$$c\dot{\sigma} + (k_1 + k_2)\sigma = ck_1\dot{\varepsilon} + k_1k_2\varepsilon$$

Solving the first-order differential equation for load yields

$$\sigma = k_1\varepsilon - \frac{k_2^{\,2}}{c} e^{-at} \int_0^t \varepsilon e^{at'} dt'$$

where

$$a = \frac{(k_1 + k_2)}{c}.$$

This equation was implemented in MatLab 6.0, making it possible to calculate the force required for a given displacement time-history if the spring and dashpot coefficients are known.

References

Ahroni, J. H., E. J. Boyko, et al. (1998). "Reliability of F-scan in-shoe measurements of plantar pressure." Foot Ankle Int **19**(10): 668-73.

Albert, S. and C. Rinole (1994). "Effect of custom orthotics on plantar pressure distribution in the pronated diabetic foot." J Foot Ankle Surg **33**: 598-604.

Bauman, W., B. Krabbe, et al. (1992). "The application of in-shoe pressure distribution measurements in the controlled therapy of diabetes patients." V.D.I. Berichte **940**: 413-419.

Harman, E., P. Frykman, et al. "A comparison of 2 current-issue Army boots, 5 prototype military boots, and 5 commercial hiking boots: performance, efficiency, biomechanics, comfort and injury." Military Performance Division, U.S. Army Institute of Environmental Medicine. Report #000427-0940.

Luo, Z. P., L. J. Berglund, et al. (1998). "Validation of F-Scan pressure sensor system: a technical note." J Rehabil Res Dev **35**(2): 186-91.

McPoil, T. G., M. W. Cornwall, et al. (1995). "A comparison of two in-shoe platnar pressure measurement systems." Lower Extremity **2**(2): 95-103.

Mueller, M. J., D. R. Sinacore, et al. (1994). "Hip and ankle walking strategies: effect on peak plantar pressures and implications for neuropathic ulceration." Arch Phys Med Rehabil **75**(11): 1196-200.

Novick, A., J. Stone, et al. (1993). "Reduction of plantar pressure with the rigid relief orthosis." J Am Podiatr Med Assoc **83**(3): 115-22.

Saltzman, C. L., K. A. Johnson, et al. (1992). "The patellar tendon-bearing brace as treatment for neurotrophic arthropathy: a dynamic force monitoring study." Foot Ankle **13**(1): 14-21.

Savelberg, H. H. and A. L. de Lange (1999). "Assessment of the horizontal, fore-aft component of the ground reaction force from insole pressure patterns by using artificial neural networks." Clin Biomech (Bristol, Avon) **14**(8): 585-92.

Sih, B. L. (2001). "A portable F-scan system." Simulation, Engineering, and Testing Group, Jaycor, Inc., San Diego, CA. Report #3150-32-01-145.

Sumiya, T., Y. Suzuki, et al. (1998). "Sensing stability and dynamic response of the F-Scan in-shoe sensing system: a technical note." J Rehabil Res Dev **35**(2): 192-200.

Woodburn, J. and P. S. Helliwell (1996). "Observations on the F-scan in-shoe pressure measuring system." Clin Biomech **11**: 301-5.